

Supporting Information

Acetylcysteine-Functionalized Microporous Conjugated Polymers for Potential Separation of Uranium from Radioactive Effluents

Xiaoli Han, Meiyun Xu, Sen Yang, Jun Qian, Daoben Hua

^a School for Radiological and Interdisciplinary Sciences (RAD-X) & College of Chemistry, Chemical Engineering and Materials Science, Soochow University, Suzhou 215123, China

^b Collaborative Innovation Center of Radiological Medicine of Jiangsu Higher Education Institutions, Suzhou 215123, China

Table of contents

Characterization methods.....	S2
Sorption kinetics.....	S2
Sorption isotherms.....	S3
Distribution ratio (K_d).....	S3
Table S1.....	S4
Table S2.....	S5
Table S3.....	S5
Table S4.....	S6
Table S5.....	S6
Fig. S1.....	S7
Fig. S2.....	S7
Fig. S3.....	S8
Fig. S4.....	S8
Fig. S5.....	S9
Fig. S6.....	S9
Fig. S7.....	S10
Fig. S8.....	S10
Fig. S9.....	S11
References.....	S11

1. Characterization methods

Infrared absorption spectra were acquired by a Varian-1000 Fourier transform infrared (FT-IR) spectrometer. Solid-state ^{13}C CP/MAS NMR measurements were carried out on a Bruker Avance III model 400 MHz NMR spectrometer at a MAS rate of 5 kHz. Elemental analysis (EA) was determined by ELEMENTAR CHNOS Elemental Analyzer. The uranyl ions concentration was determined by thermo high resolution inductively coupled plasma mass spectrometer (ICP-MS, Element II). Surface areas and pore size distributions were measured by nitrogen sorption and desorption at 77.3 K using the ASAP 2020 volumetric sorption analyzer. BET surface areas were calculated over the relative pressure range 0.05-0.15 P/P₀. Samples were degassed at 100 °C for 10 h under high vacuum before analysis. ^{60}Co gamma-ray irradiation was carried out at ^{60}Co radiation laboratory of Soochow University. The dose rate was 15 Gy/min. Malvern Zeta sizer (632.8 nm, He-Ne laser) was used to record the zeta potential and Z-average size distribution of the corresponding materials.

2. Sorption kinetics

Pseudo-first-order equation is described as followed (1):

$$\log(q_e - q_t) = \log q_e - \left(\frac{k_1}{2.303}\right) \times t \quad (1)$$

where q_e and q_t (mg/g) are the sorption capacity of U(VI) at equilibrium time and contact time t (min), respectively, and k_1 (min^{-1}) represents the pseudo first order kinetic constant. q_e and k_1 can be calculated from the slope and intercept of the plot of $\log (q_e - q_t)$ versus t , respectively (Fig. S7A).

Pseudo-second-order model is expressed as the following Equation (2):

$$\frac{t}{q_t} = \frac{1}{k_2 \times q_e^2} + \frac{t}{q_e} \quad (2)$$

where k_2 (g/mg/min) represents the rate constant of the pseudo-second order model, and can be determined from the plot of t/q_t against t (Fig. S7B).

3. Sorption isotherms

Langmuir model can be described as Equation (3):

$$\frac{C_e}{q_e} = \frac{1}{q_{\max} b} + \frac{C_e}{q_{\max}} \quad (3)$$

where b (L/mg) is the Langmuir constant related to the affinity of binding sites, and q_{\max} (mg/g) is the maximum sorption capacity. They can be calculated from the linear plot of C_e/q_e against C_e (Fig. S8A and S9A).

The Freundlich model¹ is applied for multilayer sorption, which can be described as Equation (4):

$$\log q_e = \log K_F + \frac{1}{n} \log C_e \quad (4)$$

where K_F [mg/g (L/mg)^{1/n}] and n are the Freundlich constants related to sorption capacity and sorption intensity, respectively, which can be calculated from the linear plot of $\log q_e$ versus $\log C_e$ (Fig. S8B and S9B).

4. Distribution ratio (K_d)

The distribution ratio (K_d) is calculated according to Equation (5):

$$K_d = \frac{C_0 - C_e}{C_e} \times \frac{V}{M} \quad (5)$$

where C_0 and C_e (mg/L) are the initial and equilibrium concentration of uranyl ions, respectively. M

(g) is the weight of sorbent, and V (L) is the volume of the testing solution.

Table S1. Comparison of sorption rate and sorption capacity of U(VI) on various uranium sorbents.

Sorbents	Experimental conditions	Sorption equilibration time	Sorption capacity (mg/g)	References
Fe ₃ O ₄ @SiO ₂ -AO	pH 5.0, T 298 K	4h	104	1
Amino functional MOFs	pH 5.5, T 298 K	50min	350	2
Poly(acrylic acid)-functionalized microspheres	pH 4.5, T 298 K	2.5h	990	3
GO-ACF	pH 5.5, T 298 K	1h	394	4
SBA-15	pH 4.0, T 298 K	3h	65	5
Mesoporous carbon	pH 4.0, T 298 K	5min	67	6
MA-TMA	pH 4.5, T 298 K	10min	324	7
Benzimidazole-functionalized 2D COF	pH 4.5, T 298 K	30min	211	8
MCP-3	pH 5.5, T 298 K	40s	165	This work

Table S2. Kinetic parameters for the sorption of U(VI) by MCP-1,2,3,4. (Experimental condition: 1 mg of sorbent dose, 5 mL of solution, 1×10^{-5} mol/L U(VI), pH 5.5 ± 0.1 , and 298.15 K.)

Material	Pseudo-first order				Pseudo-second order		
	$q_{e,exp}$ (mg/g)	k_1 (/min)	$q_{e,cal}$ (mg/g)	R^2	k_2 (g/mg/min)	$q_{e,cal}$ (mg/g)	R^2
MCP-1	5.616	0.187	0.579	0.789	0.352	5.624	0.999
MCP-2	5.895	0.082	0.495	0.421	1.983	5.885	0.999
MCP-3	6.473	0.061	0.173	0.148	6.759	6.468	0.999
MCP-4	7.051	0.512	1.014	0.786	2.880	7.063	0.999

Table S3. Langmuir and Freundlich parameters for U(VI) sorption by the MCPs. (Experimental conditions: 1 mg of sorbent dose, 5 ml of solution, 4.2×10^{-5} mol/L $\sim 4.2 \times 10^{-4}$ mol/L U(VI), pH 5.5 ± 0.1 , and 298.15 K , contact time = 20 min)

Material	Langmuir			Freundlich		
	q_{max} (mg/g)	b (L/mg)	R^2	K_F (L/g)	n	R^2
MCP-1	64.26	0.0687	0.994	2.83	2.025	0.973
MCP-2	112.17	0.0834	0.994	4.62	2.565	0.982
MCP-3	165.25	0.6673	0.998	8.71	5.089	0.976
MCP-4	70.11	0.3978	0.995	5.54	4.948	0.931

Table S4. Langmuir and Freundlich parameters for U(VI) sorption by the MCPs. (Experimental conditions: 1 mg of sorbent dose, 5 ml of solution, 4.2×10^{-6} mol/L $\sim 4.2 \times 10^{-5}$ mol/L U(VI), pH 5.5 \pm 0.1, and 298.15 K, contact time = 20 min.)

Material	Langmuir			Freundlich		
	q_{max} (mg/g)	b (L/mg)	R^2	K_F (L/g)	n	R^2
MCP-1	17.67	2.8931	0.962	3.42	2.787	0.991
MCP-2	28.94	4.9076	0.966	4.95	2.246	0.992
MCP-3	23.59	51.060	0.892	5.23	3.656	0.992
MCP-4	23.94	33.677	0.919	5.10	3.658	0.990

Table S5. Comparison of the diameter of coexisting ions in the solution.*

Species	$(\text{UO}_2)_3(\text{OH})_5^+$	$(\text{UO}_2)_4(\text{OH})_7^+$	OH^-	NO_3^-	Cr^{3+}	Co^{2+}	Ni^{2+}	Cd^{2+}	Nd^{3+}	Zn^{2+}
Size (nm)	1.2	1.5	0.1 1	0.33	0.14	0.15	0.13	0.19	0.19	0.15

*: The data for metal ions was from Periodic Table of Chemical Elements. Anions and uranyl complexes were simulated by Chem 3D software and CrystalMaker Demo (Fig. S6†), respectively.

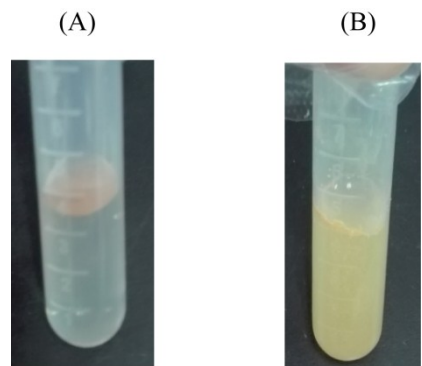


Fig. S1 Dispersibility of MCP-0 (A) and MCP-1 (B) in water.

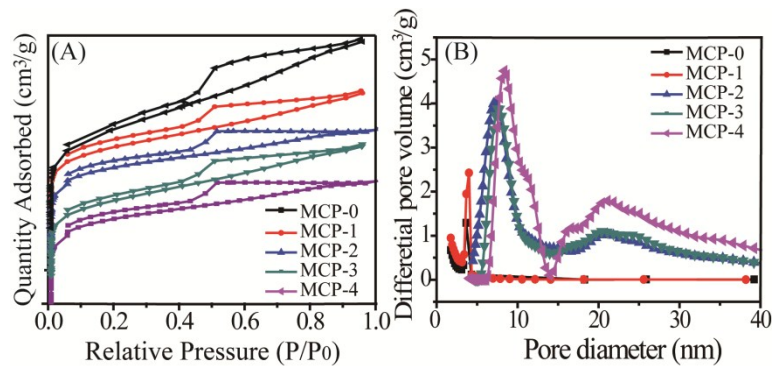


Fig. S2 (A) Nitrogen sorption (the bottom line) /desorption (the above line) isotherms and (B) pore size distribution for MCP-0, 1, 2, 3, 4.

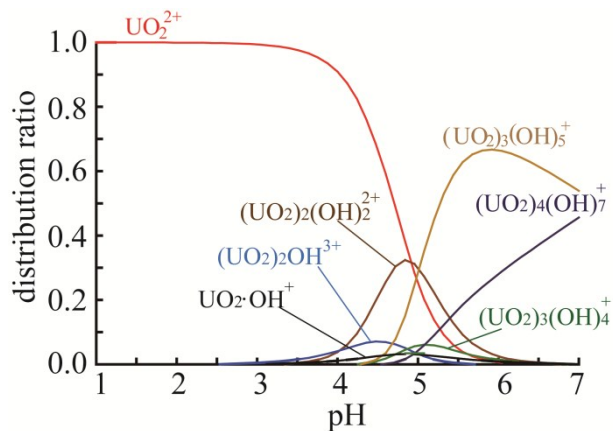


Fig. S3 Distribution of U(VI) species in aqueous solution ($[U] = 0.67\text{mmol/L}$ and pH values ranging from 1 to 7), which was simulated by Medusa program.

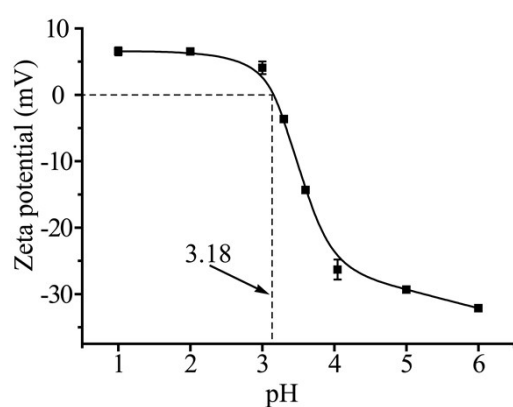


Fig. S4 Zeta potential of MCP-1.

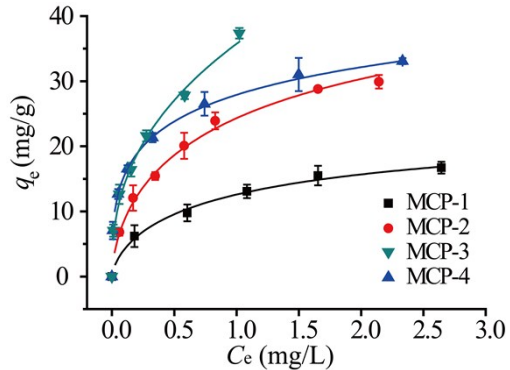


Fig. S5 Sorption isotherms of U(VI) on MCPs. (Experimental condition: 1 mg of sorbent dose, 5 mL of solution, 4.2×10^{-6} mol/L $\sim 4.2 \times 10^{-5}$ mol/L U(VI), pH 5.5 ± 0.1 , and 298.15 K.)

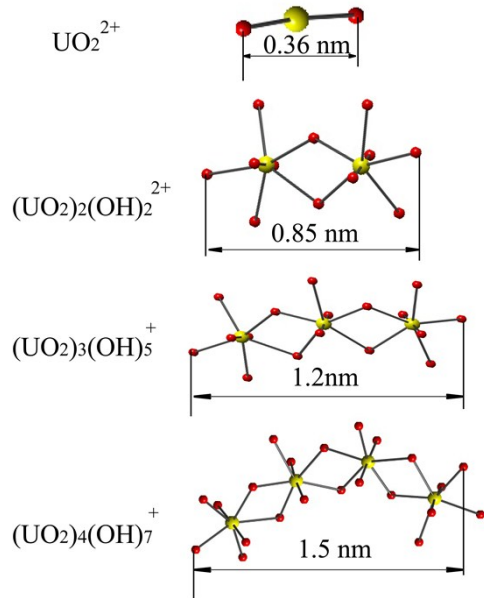


Fig. S6 The diameter of the uranium species by CrystalMaker Demo.

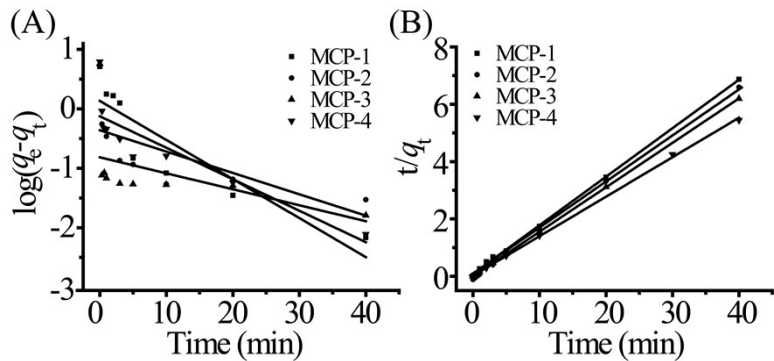


Fig. S7 (A) Pseudo-first order kinetics and (B) pseudo-second order kinetics for the sorption of U(VI) onto the MCPs.

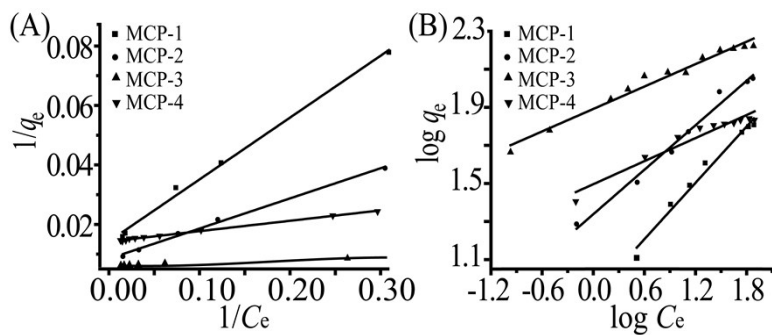


Fig. S8 (A) Langmuir sorption isotherm plots and (B) Freundlich sorption isotherm plots for the sorption of U(VI) onto the MCPs.

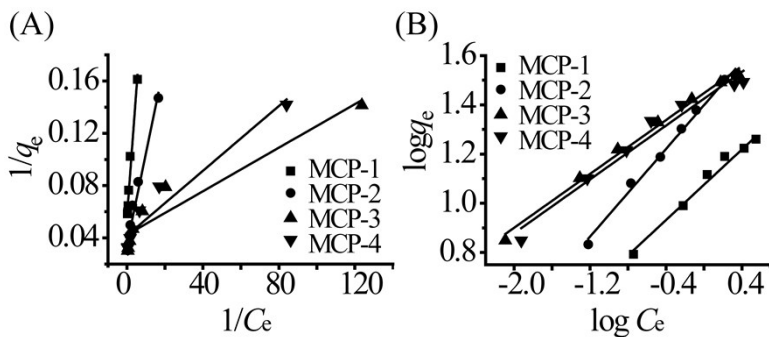


Fig. S9 (A) Langmuir sorption isotherm plots and (B) Freundlich sorption isotherm plots for the sorption of U(VI) onto the MCPs. (Experimental condition: 1 mg of sorbent dose, 5 mL of solution, 4.2×10^{-6} mol/L ~ 4.2×10^{-5} mol/L U(VI), pH 5.5 ± 0.1 , and 298.15 K.)

References

- Y. G. Zhao, J. X. Li, L. P. Zhao, S. W. Zhang, Y. S. Huang, X. L. Wu and X. K. Wang, *Chemical Engineering Journal*, 2014, **235**, 275-283.
- Z. Q. Bai, L. Y. Yuan, L. Zhu, Z. R. Liu, S. Q. Chu, L. R. Zheng, J. Zhang, Z. F. Chai and W. Q. Shi, *Journal of Materials Chemistry A*, 2015, **3**, 525-534.
- S. Zhang, X. W. Shu, Y. Zhou, L. Huang and D. B. Hua, *Chemical Engineering Journal*, 2014, **253**, 55-62.
- Y. Wang, Z. S. Wang, Z. X. Gu, J. J. Yang, J. L. Liao, Y. Y. Yang, N. Liu and J. Tang, *Journal of Radioanalytical and Nuclear Chemistry*, 2015, **304**, 1329-1337.
- Y. L. Wang, L. J. Song, L. Zhu, B. L. Guo, S. W. Chen and W. S. Wu, *Dalton Transactions*, 2014, **43**, 3739-3749.
- M. Carboni, C. W. Abney, K. M. L. Taylor-Pashow, J. L. Vivero-Escoto and W. B. Lin, *Industrial & Engineering Chemistry Research*, 2013, **52**, 15187-15197.
- B. Li, C. Y. Bai, S. Zhang, X. S. Zhao, Y. Li, L. Wang, K. Ding, X. Shu, S. J. Li and L. J. Ma, *Journal of Materials Chemistry A*, 2015, **3**, 23788-23798.
- J. Li, X. D. Yang, C. Y. Bai, Y. Tian, B. Li, S. Zhang, X. Y. Yang, S. D. Ding, C. Q. Xia, X. Y. Tan, L. J. Ma and S. J. Li, *Journal of Colloid and Interface Science*, 2015, **437**, 211-218.